Materials Science & Engineering B 250 (2019) 114424

Contents lists available at ScienceDirect

Materials Science & Engineering B

journal homepage: www.elsevier.com/locate/mseb

A novel temperature stable $Mg_{0.5}Ti_{0.5}NbO_4$-based microwave dielectric material

Liping Zhao[a], Peng Liu[a,*], Zhifen Fu[a,b]

[a] College of Physics and Information Technology, Shaanxi Normal University, Xi'an 710062, China
[b] College of Science, Anhui University of Science and Technology, Huainan 232001, China

ARTICLE INFO

Keywords:
$Mg_{0.5}Ti_{0.5}NbO_4$-based ceramics
Microstructure
X-ray diffraction
Microwave dielectric properties

ABSTRACT

A novel temperature stable $Mg_{0.5}Ti_{0.5}NbO_4$-based microwave dielectric ceramic was fabricated by using the nanopowders (317 nm) derived from high energy ball milling (HEBM) method. An orthorhombic ixiolite structure was detected for $Mg_{0.5}Ti_{0.5}NbO_4$ ceramics coupled with a minor of second phase $Mg_{0.167}Nb_{0.33}Ti_{0.5}O_2$. With increasing sintering temperature, the amount of $Mg_{0.167}Nb_{0.33}Ti_{0.5}O_2$ phase decreased as well as the dielectric constant (ε_r) and temperature coefficient of resonant frequency (τ_f). The ceramics sintered at 1140 °C for 4 h exhibited optimum microwave dielectric properties $\varepsilon_r = 38.8$, $Q \times f = 19{,}710$ GHz and $\tau_f = 1.3$ ppm/°C.

1. Introduction

The rapid development of wireless communication technology has stimulated the development of the microwave dielectric ceramics, which are widely used by microwave components such as oscillators, resonators, duplexers, filters etc [1–4]. Many researchers are paying attention to develop new microwave dielectric ceramics with moderate dielectric constant ($\varepsilon_r \sim 40$), low dielectric loss ($Q \times f \sim 10{,}000$–$60{,}000$ GHz) and near-zero temperature coefficient of resonant frequency (τ_f) due to the carrier frequency of interest in communication systems was extended from GSM 900 MHz to ISM bands (2.4, 5.2, and 5.8 GHz) or even to the millimeter wave range [5,6]. As early as 1994, H. Kagata et al. reported $Ca(A_{1/2}Nb_{1/2})O_3$ (A = Fe, Zn) ceramics with medium dielectric constant exhibited good microwave dielectric properties: $\varepsilon_r = 40$ and 35, $Q \times f = 20{,}000$ and 16,000 GHz and $\tau_f = -76$ and -43 ppm/°C, respectively [7]. These microwave dielectric ceramics with $\varepsilon_r \sim 40$ have one common drawback: the τ_f is relatively large.

Recent years, $A_{0.5}Ti_{0.5}NbO_4$ (A = Ni, Zn, Co and Cu) [8–12] microwave dielectric ceramics with $\varepsilon_r \sim 40$ have been focused due to their flexibility about the substitution of different A-site cations. Liao et al. firstly investigated the microwave dielectric properties of tetragonal rutile structure $Ni_{0.5}Ti_{0.5}NbO_4$ ($\varepsilon_r = 56.8$, $Q \times f = 21{,}100$ GHz and $\tau_f = +79.1$ ppm/°C) [8]. C.F. Tseng reported that tetragonal rutile structure $A_{0.5}Ti_{0.5}NbO_4$ (A = Co and Cu) exhibited excellent microwave dielectric properties of $\varepsilon_r = 64$ and 71.2, $Q \times f = 65{,}300$ and 11,000 GHz and $\tau_f = +223.2$, and + 49.2 ppm/°C, respectively [9,10]. The $Zn_{0.5}Ti_{0.5}NbO_4$ ceramics with orthorhombic ixiolite structure showed excellent microwave dielectric properties of $\varepsilon_r = 37.4$, $Q \times f = 194{,}000$ GHz and $\tau_f = -58$ ppm/°C [9]. These ceramics have opposite τ_f due to their different structures. And the $Q \times f$ values of $Zn_{0.5}Ti_{0.5}NbO_4$ ceramics is an order of magnitude higher than others with $\varepsilon_r \sim 40$. The ionic radius of Mg^{2+} (0.72 Å) is similar to that of Ni^{2+} (0.69 Å) and Zn^{2+} (0.74 Å) [13]. It is worthwhile to synthesize $Mg_{0.5}Ti_{0.5}NbO_4$ new compound and investigate their dielectric properties.

In this paper, the novel $Mg_{0.5}Ti_{0.5}NbO_4$-based ceramics were fabricated, and the sintering behavior, crystal phase, microstructure and microwave dielectric properties of the material were investigated.

2. Experimental procedures

The $Mg_{0.5}Ti_{0.5}NbO_4$-based ceramics were prepared by a high energy ball milling method from the oxide powders of MgO (99.99%), TiO_2 (99.99%) and Nb_2O_5 (99.99%). The raw materials MgO(99.99%), TiO_2(99.99%) and Nb_2O_5(99.99%) with a molar ratio of 1:1:1 were milled for 10 h with Fritsch Vario–Planetary Mill (Pulverisette 4). A zirconium dioxide vial with a diameter of 80 mm and zirconium dioxide balls with diameter of 2.5, 5, 10, and 20 mm were used as milling medium. The rotational speed of vials was set at 300 rpm, and the mass ratio of ball, powder, and deionized water was 20:1:2. After milling, the mixtures were dried and calcined at 900 °C for 3 h with heating rates 2 °C/min. Subsequently, the calcined powders were reground for 10 h. After drying, the powders mixed with 5 wt% PVA as a binder and

* Corresponding author.
E-mail address: liupeng@snnu.edu.cn (P. Liu).

https://doi.org/10.1016/j.mseb.2019.114424
Received 28 March 2018; Received in revised form 8 July 2019; Accepted 9 September 2019

granulated. Next, the powders were uniaxially pressed into pellets with 11.5 mm in diameter and 5–6 mm in height under the pressure of 200 MPa. These pellets were sintered at 1060–1180 °C for 4 h with a temperature-ramping rate of 2 °C/min.

The reaction processes were investigated by thermal gravimetric and differential thermal analysis (TG/DTA) (SDT Q600 V8.0 Build 95, American) with a heating rate of 20 °C/min in air from room temperature to 1200 °C. The crystal structures of specimens were analyzed via X-ray diffraction (XRD, Rigaku D/MAX-2400, Japan) with Cu Kα radiation generated at 40 kV and 100 mA. The microstructures and grain size of the powders and ceramics were investigated using a scanning electron microscope (SEM, Fei Nova 650, Hillsboro, US), coupled with energy dispersive spectroscopy (EDS), and laser particle size analyzer (BI-90Plus, America), respectively. The bulk densities of the sintered samples were measured by the Archimedes method. The microwave dielectric properties of the specimens were measured using a network analyzer (ZVB20, Rohde & Schwarz, Munich, Germany) with the $TE_{0.1\delta}$ shielded cavity method. Temperature coefficients of resonant frequency (τ_f) were measured in the temperature range of 20–80 °C.

3. Results and discussion

The TG/DTA analysis of $MgO–TiO_2–Nb_2O_5$ powders milled for 10 h with increasing temperatures is plotted in Fig. 1. The first relatively wide endothermic peak appeared at around 223 °C, which is accompanied by a weight loss of approximately 2.2% due to the loss of hydration water [14]. The second endothermic peak at temperature about 407 °C represented the decomposition of $MgO–H_2O$ [15], which is in consistent with the second fall of weight (1.8%). The DTA curve exhibited the first exothermic peak at approximately 558 °C combined with a weight loss of 0.6%, which is related to the synthesis of $Mg_{0.5}Ti_{0.5}NbO_4$ phase. Hence, calcination temperatures were determined to be higher than 558 °C.

Fig. 2 shows X-Ray diffraction patterns of $MgO–TiO_2–Nb_2O_5$ powders calcined at different temperatures for 3 h. The uncalcined powders were composed by mixtures of MgO (Tetragonal, PDF#45-0946), Nb_2O_5 (Hexagonal, PDF#12-0104) and TiO_2 (Tetragonal, PDF#73-1232). After the mixture was calcined at 600 °C, a minor of $Mg_{0.5}Ti_{0.5}NbO_4$ was synthesized as $MgO + Nb_2O_5 + TiO_2 \rightarrow 2\,Mg_{0.5}Ti_{0.5}NbO_4$, which is consistent with the DTA analysis. When the calcination temperature was increased to 800 °C, the intensity of $Mg_{0.5}Ti_{0.5}NbO_4$ reflection peaks increased with appearance of $Ti_2Nb_{10}O_{29}$ phase ($5Nb_2O_5 + 2TiO_2 \rightarrow Ti_2Nb_{10}O_{29}$). As the calcinating temperature increased up to 900 °C, the $Mg_{0.5}Ti_{0.5}NbO_4$ phase became

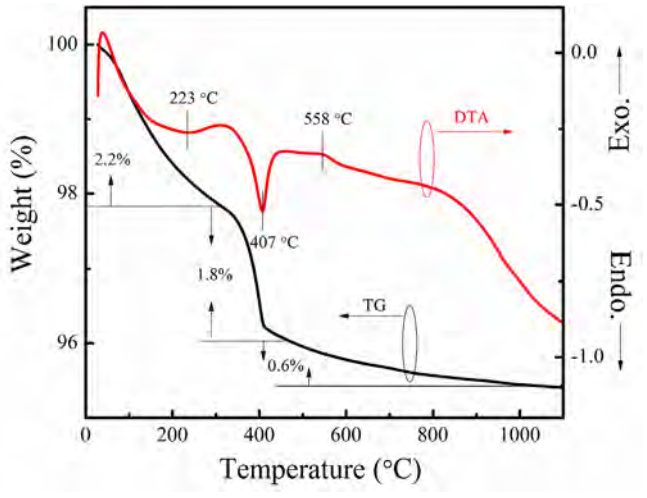

Fig. 1. TG/DTA curves of $MgO–TiO_2–Nb_2O_5$ mixture powders milled 10 h from room temperature to 1200 °C.

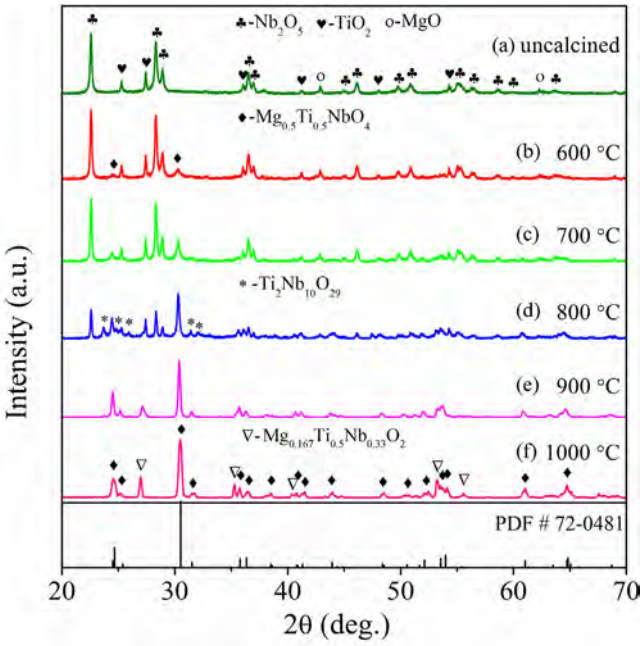

Fig. 2. XRD patterns of $MgO–TiO_2–Nb_2O_5$ mixtures powders calcined at different temperatures.

predominant phase, whose diffraction patterns matched with those of $NiNb_2O_6$ (JCPDS#72-0481), while small amount of $Ti_{0.5}Mg_{0.167}Nb_{0.33}O_2$ phase (JCPDS#40-0366) was formed ($Nb_2O_5 + MgO + 3TiO_2 \rightarrow 6Ti_{0.5}Mg_{0.167}Nb_{0.33}O_2$). The phase constitution no longer changed after 900 °C, so calcination temperature was determined as 900 °C.

The SEM micrographs and particle size distributions of $MgO–TiO_2–Nb_2O_5$ mixtures milled 10 h and those powders calcined at 900 °C are demonstrated in Fig. 3. As shown in Fig. 3(a) and (c), two SEM images exhibited a similar and uniform morphology. The average particle size of uncalcined powders and those calcined at 900 °C is to be 172 nm (Fig. 3(b)) and 317 nm (Fig. 3(d)), respectively.

Fig. 4 presents the XRD patterns of $Mg_{0.5}Ti_{0.5}NbO_4$-based powders calcined at 900 °C for 3 h and ceramics sintered at various temperatures. The diffraction patterns closely matched with that of orthorhombic ixiolite structure $NiNb_2O_6$ ceramics with space group Pbcn (60), which is similar to $Mg_{0.5}Zn_{0.5}TiNb_2O_8$ [2] and $MgTiNb_2O_8$ [16]. In addition, secondary phase of $Mg_{0.167}Nb_{0.33}Ti_{0.5}O_2$ with space group P42/mnm (1 3 6) existed in all samples. As shown in Fig. 2(b–f), with increasing temperature, the intensity of $Mg_{0.167}Nb_{0.33}Ti_{0.5}O_2$ diffraction peaks was weakened, which is effective to modify the τ_f value of $Mg_{0.5}Ti_{0.5}NbO_4$ ceramics to 0 ppm/°C.

The surface SEM images of $Mg_{0.5}Ti_{0.5}NbO_4$-based ceramics sintered at temperatures from 1100 to 1180 °C are demonstrated in Fig. 5(a–d). It can be seen that all specimens exhibited a similar morphology with two kinds of grains, bigger grains A and smaller grains B. Based on the EDS analyses (Fig. 5(e, f)), the grains A and B were considered to be $Mg_{0.5}Ti_{0.5}NbO_4$ and $Mg_{0.167}Nb_{0.33}Ti_{0.5}O_2$ respectively. As shown in Fig. 5(a), sintered at 1100 °C for 4 h, some pores existing in microstructure could be observed. With increasing temperature to 1140 °C, the well dense microstructures were obtained (Fig. 5(b)). The grain size of $Mg_{0.5}Ti_{0.5}NbO_4$ increased with sintering temperature. As the sintering temperature reached to 1180 °C, grains began to melt and the abnormal growth of grain size was appeared (Fig. 5(d)). From 1100 °C to 1180 °C, the grain size of $Mg_{0.167}Nb_{0.33}Ti_{0.5}O_2$ nearly unchanged and the quantity was significantly decreased, which is consistent with the XRD results in Fig. 4.

Fig. 6 exhibits the bulk density, dielectric constant (ε_r), quality factor ($Q \times f$), and temperature coefficient of resonant frequency (τ_f)

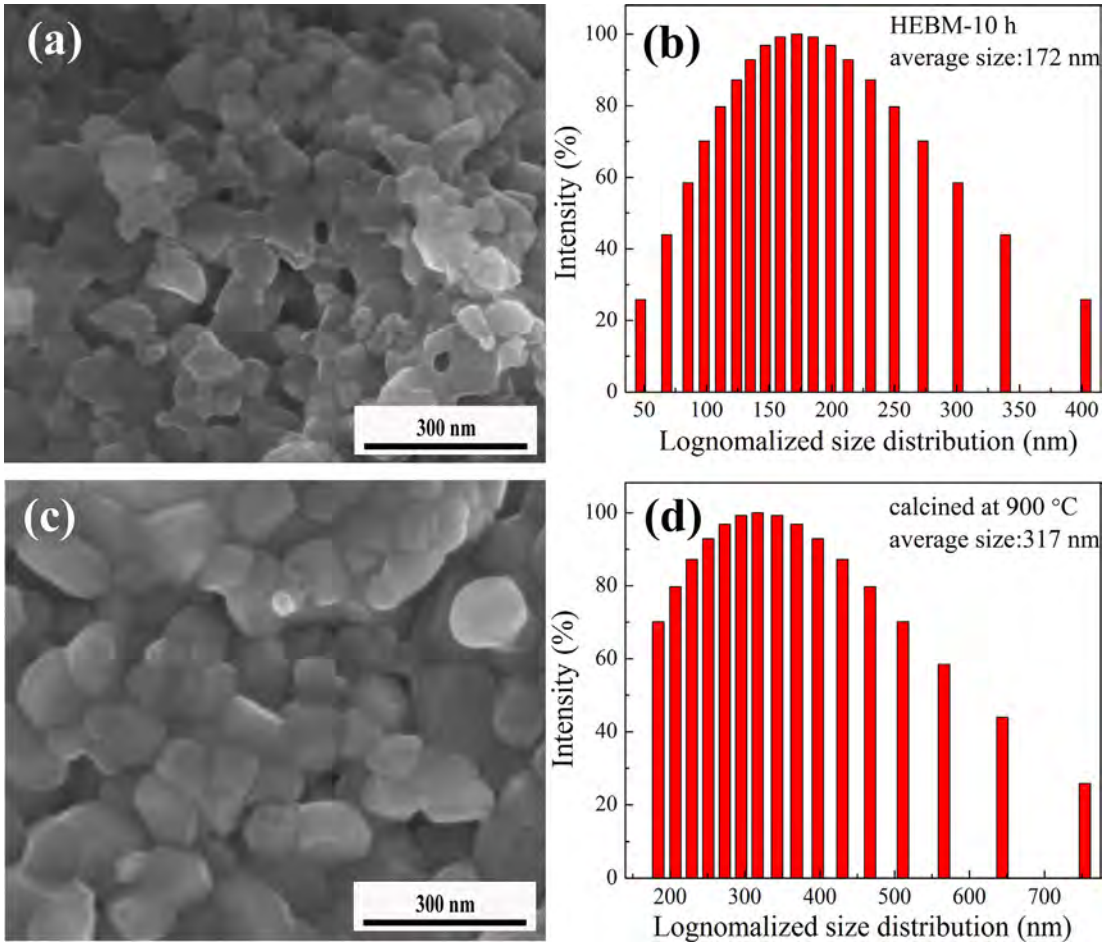

Fig. 3. SEM micrographs of $MgO–TiO_2–Nb_2O_5$ mixtures: (a) uncalcined and (b) calcined at 900 °C; and particle size distributions of the mixtures: (c) uncalcined and (d) calcined at 900 °C.

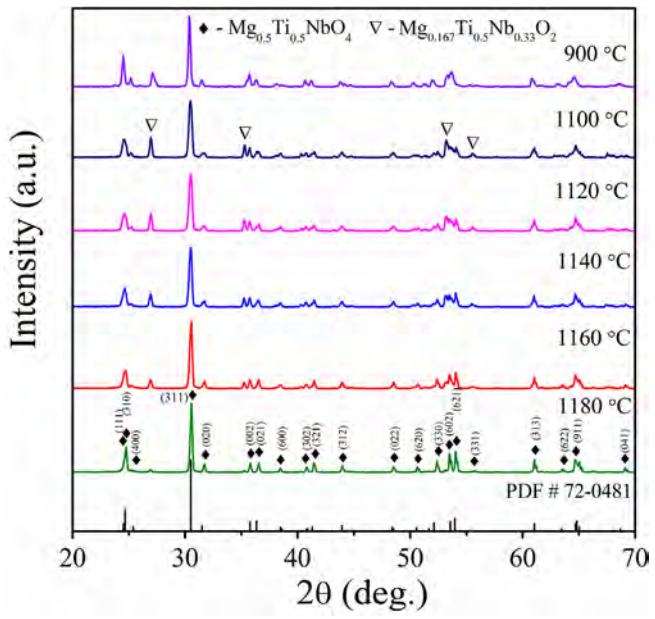

Fig. 4. XRD patterns of $Mg_{0.5}Ti_{0.5}NbO_4$-based powders calcined at 900 °C for 3 h and ceramics sintered at various temperatures.

values of $Mg_{0.5}Ti_{0.5}NbO_4$-based ceramics as a function of sintering temperatures. As shown in Fig. 6(a), with increasing sintering temperature, the density of samples firstly increased and reached to maximum value of 4.8 g/cm^3 at 1140 °C. After then, it decreased with further increasing of the sintering temperature, which may be attributed to the changes of phase constitutions and abnormal grain growth [17]. As far as we know, the microwave dielectric properties of secondary phase $Mg_{0.167}Nb_{0.33}Ti_{0.5}O_2$ ceramic have not been investigated. So, the ceramic was prepared with microwave dielectric properties of $\varepsilon_r = 77$, $Q \times f = 9719$ GHz, $\tau_f = +268$ ppm/°C, which is comparable to those of $Zn_{0.17}Nb_{0.33}Ti_{0.5}O_2$ ($\varepsilon_r = 95$, $Q \times f = 15{,}000$ GHz, $\tau_f = +237$ ppm/°C) [18,19]. The relationships between $Q \times f$ values and sintering temperature follow a similar trend with that between bulk density and sintering temperature in Fig. 6(b). As sintering temperature increases, $Q \times f$ values increased from 12,600 to 19,710 GHz and then decreased to 15,090 GHz, owing to the secondary phase and the abnormal grain growth [17]. As we all know, the permittivity is dependent on the density, secondary phases, and the crystal structure in microwave frequency [20]. As shown in Fig. 6(a), ε_r values versus sintering temperature showed a trend of decrease from 39.9 to 33.1 in temperature rang of 1100–1180 °C. The decrease of ε_r values was mainly related to the decrease of secondary phase $Mg_{0.167}Nb_{0.33}Ti_{0.5}O_2$ with ε_r values of 77. The composition, secondary phases, and additives of the material are generally known to affect the τ_f values [9]. The τ_f values showed a trend of decrease from 24.5 to −57.1 ppm/°C with increase of sintering temperature from 1100 to 1180 °C in Fig. 6(b) due to the decrease of $Mg_{0.167}Nb_{0.33}Ti_{0.5}O_2$ possessing τ_f value of 268 ppm/°C. A near–zero τ_f value of 1.3 ppm/°C was obtained at 1140 °C. Compared to the other developed microwave dielectrics ceramics with $\varepsilon_r \sim 40$, the present material with near zero τ_f value was obtained conventionally.

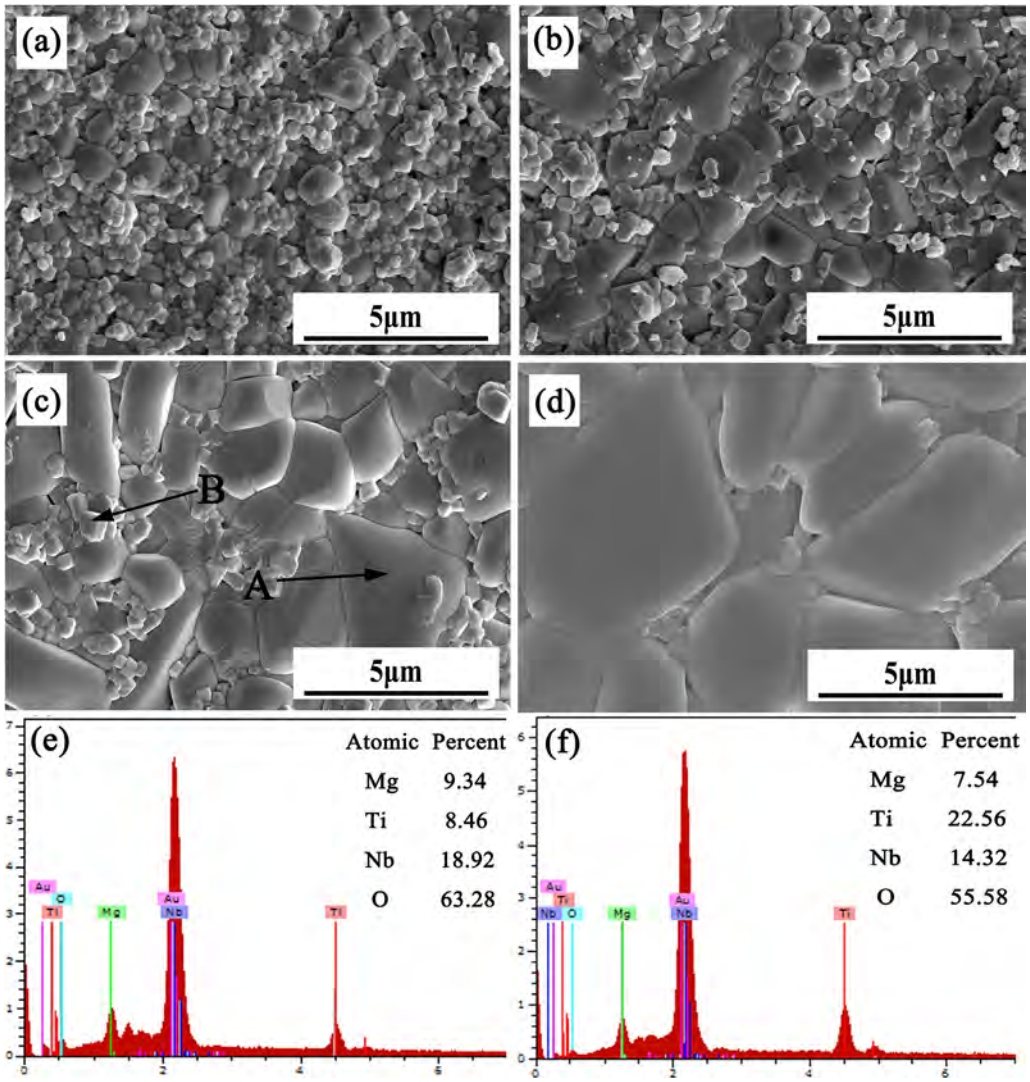

Fig. 5. SEM micrographs of $Mg_{0.5}Ti_{0.5}NbO_4$ ceramics sintered at (a) 1100 °C, (b) 1140 °C, (c) 1160 °C and (d) 1180 °C, and EDS spectrums of spot A and B marked in (c).

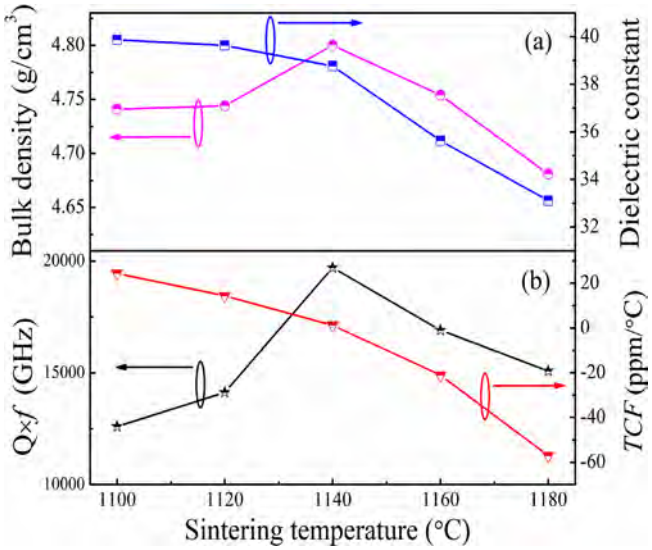

Fig. 6. (a) Bulk density and dielectric constant (ε_r), (b) quality factor ($Q \times f$) and τ_f of the $Mg_{0.5}Ti_{0.5}NbO_4$-based ceramics sintered at 1100–1180 °C.

4. Conclusions

$Mg_{0.5}Ti_{0.5}NbO_4$-based powders with an average grain size of 317 nm were obtained by high energy ball milling method. The ceramics showed a orthorhombic ixiolite structure with a minor of second phase $Mg_{0.167}Nb_{0.33}Ti_{0.5}O_2$. With increasing sintering temperature from 1100 to 1180 °C, the amount of second phase was decreased as well as the ε_r and τ_f shifted from 39.9 and 24.5 ppm/°C to 33.1 and −57.1 ppm/°C, respectively. When sintered at 1140 °C, the new dielectric ceramic with dense microstructure exhibited good microwave dielectric properties: $\varepsilon_r = 38.8$, $Q \times f = 19{,}710$ GHz and $\tau_f = 1.3$ ppm/°C. The novel material is an attractive candidate of temperature stable microwave dielectrics application.

Declaration of Competing Interest

The authors declare that they have no known competing financial interests or personal relationships that could have appeared to influence the work reported in this paper.

Acknowledgment

This work is supported by the National Natural Science Foundation

of China (Grant No: 51572162, 51602005).

References

[1] H. Ohsato, Research and development of microwave dielectric ceramics for wireless communications, J. Ceram. Soc. Jpn. 113 (1323) (2005) 703–711.

[2] Q. Liao, L. Li, X. Ding, et al., A new temperature stable microwave dielectric material $Mg_{0.5}Zn_{0.5}TiNb_2O_8$, J. Am. Ceram. Soc. 95 (5) (2012) 1501–1503.

[3] C.L. Huang, Y.W. Tseng, J.Y. Chen, et al., Dielectric properties of high-Q $(Mg_{1-x}Zn_x)_{1.8}Ti_{1.1}O_4$ ceramics at microwave frequency, J. Eur. Ceram. Soc. 32 (10) (2012) 2365–2371.

[4] E. Nenasheva, S. Redozubov, N. Kartenko, et al., Microwave dielectric properties and structure of $ZnO–Nb_2O_5–TiO_2$ ceramics, J. Eur. Ceram. Soc. 31 (6) (2011) 1097–1102.

[5] C.L. Huang, J.Y. Chen, High-Q microwave dielectrics in the $(Mg_{1-x}Co_x)_2TiO_4$ ceramics, J. Am. Ceram. Soc. 92 (2) (2009) 379–383.

[6] X. Lyu, L. Li, S. Zhang, et al., A new low-loss dielectric material $ZnZrTa_2O_8$ for microwave devices, J. Eur. Ceram. Soc. 36 (3) (2016) 931–935.

[7] H. Kagata, J. Kato, Dielectric properties of Ca-based complex perovskite at microwave frequencies, Jpn. J. Appl. Phys. 33 (9S) (1994) 5463.

[8] Q. Liao, L. Li, X. Ren, et al., A new microwave dielectric material $Ni_{0.5}Ti_{0.5}NbO_4$, Mater. Lett. 89 (2012) 351–353.

[9] C.F. Tseng, Microwave dielectric properties of low loss microwave dielectric ceramics: $A_{0.5}Ti_{0.5}NbO_4$ (A = Zn, Co), J. Eur. Ceram. Soc. 34 (15) (2014) 3641–3648.

[10] C.F. Tseng, Microwave dielectric properties of a new $Cu_{0.5}Ti_{0.5}NbO_4$ ceramics, J. Eur. Ceram. Soc. 35 (1) (2015) 383–387.

[11] J. Bi, C. Yang, Wu.H. Synthesis, characterization, and microwave dielectric properties of $Ni_{0.5}Ti_{0.5}NbO_4$ ceramics through the aqueous sol–gel process, J. Alloys Compd. 653 (2015) 1–6.

[12] T. Chen, W. Ma, Q. Sun, et al., The microwave dielectric properties of $(Ni, Zn)_{0.5}Ti_{0.5}NbO_4$ solid solution, Mater. Lett. 113 (2013) 111–113.

[13] R.D. Shannon, Revised effective ionic radii and systematic studies of interatomic distances in halides and chalcogenides, Acta Crystallogr. Sec. A 32 (5) (1976) 751–767.

[14] F. Tavangarian, R. Emadi, Mechanical activation assisted synthesis of pure nanocrystalline forsterite powder, J. Alloys Compd. 485 (1–2) (2009) 648–652.

[15] Z.F. Fu, P. Liu, X.M. Chen, et al., Low-temperature synthesis of $Mg_4Nb_2O_9$ nanopowders by high-energy ball-milling method, J. Alloys Compd. 493 (1–2) (2010) 441–444.

[16] Q.W. Liao, Investigation on the Structure-Properties Relationship of Ultra-Low Loss AB(Nb, Ta)2_O8 Microwave Dielectric Ceramics, Tianjin University, 2012.

[17] X. Bai, P. Liu, Z. Fu, et al., $LiAlW_2O_8$: a novel temperature stable low-firing microwave dielectric ceramic, Mater. Lett. 178 (2016) 68–70.

[18] E.S. Kim, D.H. Kang, Relationships between crystal structure and microwave dielectric properties of $(Zn_{1/3}B_{2/3}^{5+})_xTi_{1-x}O_2$ (B^{5+} = Nb, Ta) ceramics, Ceram. Int. 34 (4) (2008) 883–888.

[19] M. Guo, S. Gong, G. Dou, et al., A new temperature stable microwave dielectric ceramics: $ZnTiNb_2O_8$ sintered at low temperatures, J. Alloys Compd. 509 (20) (2011) 5988–5995.

[20] P. Ruan, P. Liu, B.C. Guo, et al., Microwave dielectric properties of $ZnO–Nb_2O_5–xTiO_2$ ceramics prepared by reaction-sintering process, J. Mater. Sci. Mater. Electron. 27 (5) (2016) 4201–4205.